

F. Dong · C. X. Fang · X. Yang · X. Zhang
F. L. Lopez · J. Ren

Cardiac overexpression of catalase rescues cardiac contractile dysfunction induced by insulin resistance: role of oxidative stress, protein carbonyl formation and insulin sensitivity

Received: 21 December 2005 / Accepted: 10 February 2006 / Published online: 4 April 2006
© Springer-Verlag 2006

Abstract *Aims/hypothesis:* Insulin resistance leads to oxidative stress and cardiac dysfunction. This study examined the impact of catalase on insulin-resistance-induced cardiac dysfunction, oxidative damage and insulin sensitivity. *Methods:* Insulin resistance was initiated in FVB and catalase-transgenic mice by 12 weeks of sucrose feeding. Contractile and intracellular Ca^{2+} properties were evaluated in cardiomyocytes including peak shortening (PS), time-to-PS (TPS), time-to-90% relengthening (TR_{90}), half-width duration (HWD), maximal velocity of shortening/relengthening ($\pm\text{dL}/\text{dt}$), fura-fluorescence intensity change (ΔFFI) and intracellular Ca^{2+} clearance rate (τ). Reactive oxygen species (ROS) and protein damage were evaluated with dichlorodihydrofluorescein and protein carbonyl formation. *Results:* Sucrose-fed mice displayed hyperinsulinaemia, impaired glucose tolerance and normal body weight. Myocytes from FVB sucrose-fed mice exhibited depressed PS and $\pm\text{dL}/\text{dt}$, prolonged TR_{90} and τ , and reduced ΔFFI associated with normal TPS and HWD compared with those from starch-fed control mice. ROS and protein carbonyl formation were elevated in FVB sucrose-fed mice. Insulin sensitivity was reduced, evidenced by impaired insulin-stimulated 2-deoxy-D- ^3H glucose uptake. Western blot analysis indicated that sucrose feeding: (1) inhibited insulin-stimulated phosphorylation of insulin receptor and Akt; (2) enhanced protein-tyrosine phosphatase 1B (PTP1B) expression; and (3) suppressed endothelial nitric oxide synthase (eNOS) and $\text{Na}^+-\text{Ca}^{2+}$ exchanger expression without affecting peroxisome proliferator-activated receptor γ (PPAR γ), sarco(endo)plasmic reticulum Ca^{2+} -ATPase isozyme 2a and phospholamban. Catalase ablated insulin-resistance-

induced mechanical dysfunction, ROS production and protein damage, and reduced eNOS, but not insulin insensitivity. Catalase itself decreased resting FFI and enhanced expression of PTP1B and PPAR γ . *Conclusions/interpretation:* These data indicate that catalase rescues insulin-resistance-induced cardiac dysfunction related to ROS production and protein oxidation but probably does not improve insulin sensitivity.

Keywords Catalase · Insulin · Insulin resistance · Myocyte · Shortening · Protein carbonyl

Abbreviations $-\text{dL}/\text{dt}$: maximal velocity of relengthening · $+\text{dL}/\text{dt}$: maximal velocity of shortening · eNOS: endothelial nitric oxide synthase · HWD: half-width duration · NCX: $\text{Na}^+-\text{Ca}^{2+}$ exchanger · pAkt: phosphorylated Akt · PLB: phospholamban · PPAR γ : peroxisome proliferator-activated receptor γ · PS: peak shortening · PTP1B: protein-tyrosine phosphatase 1B · ROS: reactive oxygen species · SERCA2a: sarco(endo)plasmic reticulum Ca^{2+} -ATPase isozyme 2a · TPS: time-to-peak shortening · TR_{90} : time-to-90% relengthening · ΔFFI : fura-fluorescence intensity change · τ : (tau) intracellular Ca^{2+} clearance rate

Introduction

Metabolic syndrome characterised by obesity, hypertension and insulin resistance is a serious medical problem resulting from interactions between genetic makeup and lifestyle [1–3]. Individuals with insulin resistance exhibit a high incidence of cardiovascular diseases such as ventricular dysfunction [1–3]. Compromised heart function associated with insulin resistance is characterised by impaired cardiac efficiency, reduced ventricular function and coronary heart disease [2–7]. Many of these dysfunctions are reminiscent of those found in diabetic individuals with compromised heart function. It has been demonstrated that diabetic heart dysfunction is often characterised by prolonged action-potential duration, impaired ventricular

F. Dong · C. X. Fang · X. Yang · X. Zhang ·
F. L. Lopez · J. Ren (✉)
Division of Pharmaceutical Sciences and Center
for Cardiovascular Research and Alternative Medicine,
University of Wyoming,
1000 E. University Avenue, Department 3375,
Laramie, WY 82071, USA
e-mail: jren@uwyo.edu
Tel.: +1-307-7666131
Fax: +1-307-7662953

compliance, reduced cytosolic Ca^{2+} clearance and prolonged ventricular relaxation [8–10]. However, it has not been fully elucidated whether prediabetic insulin resistance directly predisposes hearts to these diabetic mechanical defects.

Binding of insulin to its receptor initiates tyrosine autophosphorylation of insulin receptor [11]. The metabolic effects of insulin are mediated through IRS-1/IRS-2-mediated activation of the phosphatidylinositol-3 kinase pathway [12]. Several post-insulin-receptor molecules have been indicated to play significant roles in insulin signalling, including the serine/threonine protein kinase Akt, protein-tyrosine phosphatase 1B (PTP1B), peroxisome proliferator-activated receptor γ (PPAR γ), and mammalian target of rapamycin and S6 kinase [13–15]. It has been speculated that malfunction of these signalling molecules (either dampened or hyperactivated) may contribute to development of insulin resistance [3, 16]. Therefore, this study aimed to investigate the impact of antioxidant catalase on prediabetic insulin-resistance-induced cardiac mechanical dysfunction, oxidative stress, protein damage and insulin sensitivity at the levels of glucose uptake, insulin-receptor tyrosine phosphorylation, Akt, PTP1B and PPAR γ . We also evaluated the level of endothelial nitric oxide synthase (eNOS), a down-stream target for Akt. Ample evidence has related accumulation of reactive oxygen species (ROS) to complications of diabetes and obesity [17, 18]. However, the role of oxidative stress in cardiac dysfunction under insulin resistance is essentially unknown. We used a sucrose-diet-induced insulin-resistance model with hyperinsulinaemia and hypertriglyceridaemia [5, 6, 19]. It is believed that changes in fatty acid composition and membrane fluidity may contribute to the elevated cholesterol content and cholesterol:phospholipid ratio [19]. Cardiac contractile properties, ROS, protein carbonyl formation, cardiac Ca^{2+} -regulatory proteins including sarco(endo)plasmic reticulum Ca^{2+} -ATPase isozyme 2a (SERCA2a), phospholamban (PLB) and Na^{+} - Ca^{2+} exchanger (NCX), as well as insulin-signalling molecules at both receptor and post-receptor levels, were examined in cardiomyocytes or myocardium from both sucrose-fed prediabetic insulin-resistant and starch-fed control mice.

Materials and methods

Experimental animals and induction of whole-body insulin resistance

The experimental procedure was approved by our Institutional Animal Care Committee. Four-month-old male FVB and catalase-transgenic mice (~18 g) were fed either a cornstarch or sucrose (each providing 68% of total energy) diet (Research Diets, New Brunswick, NJ, USA) for 12 weeks. Generation and identification of cardiac-specific catalase-transgenic mice were described previously [20, 21]. A primer pair derived from the myosin heavy chain promoter and rat catalase cDNA was used with the reverse

sequence of aat atc gtg ggt gac ctc aa and the forward sequence of cag atg aag cag tgg aag ga. A line with cardiac catalase activity of $1,456 \mu\text{mol min}^{-1} \text{mg}^{-1} \text{protein}$ or 60-fold of that of the wild-type mouse was used in this study. Mice were maintained with a 12-h light/12-h darkness cycle with free access to tap water.

Intraperitoneal glucose tolerance test, glucose and insulin levels

Two days prior to killing, mice were fasted for 12 h and then given an i.p. injection of glucose (2 g/kg body weight). Blood samples were drawn from the tail vein 15 min and immediately before the glucose challenge, as well as 15, 60 and 120 min thereafter. Blood glucose and insulin levels were determined using a glucose analyser and a mouse insulin ELISA kit (Linco Research, Inc., St Charles, MO, USA), respectively [19].

Isolation of mouse ventricular myocytes

Hearts were rapidly removed and perfused (at 37°C) with Krebs–Henseleit bicarbonate buffer. After perfusion, ventricles were digested with 0.9 mg/ml collagenase D (Boehringer Mannheim Biochemicals, Indianapolis, IN, USA) for 10 min before being minced and washed to remove remnant enzyme. Extracellular Ca^{2+} was added incrementally back to 1.25 mmol/l. Fresh myocytes were used within 8 h. Cell viability was approximately 70% in all animal groups. Only rod-shaped myocytes with clear edges were selected for recording of mechanical properties [21].

Cell shortening/relengthening measurements

Mechanical properties of cardiomyocytes were assessed using a SoftEdge MyoCam system (IonOptix Corporation, Milton, MA, USA) [21]. Cell shortening and relengthening were assessed using the following indices: peak shortening (PS), time-to-PS (TPS) and time-to-90% relengthening (TR_{90}), half-width duration (HWD), which reflects the duration from 50% shortening to 50% relengthening, and maximal velocities of shortening (+dL/dt) and relengthening (–dL/dt). In the case of altering stimulus frequency, the steady-state contraction was achieved (usually after the first five or six beats) before PS was recorded.

Intracellular Ca^{2+} transient measurement

A separate cohort of myocytes was loaded with fura-2/AM (0.5 $\mu\text{mol/l}$) for 10 min and fluorescence measurements were recorded with a fluorescence photomultiplier system (IonOptix). Electrically paced (0.5 Hz) cells were exposed to light emitted by a 75 W lamp and passed through either a 360 or a 380 nm filter. Fluorescence emissions were

Table 1 General features of starch- and sucrose-fed FVB and catalase (CAT)-transgenic mice

Mouse group	Body weight (g)	Heart weight (mg)	Heart weight/body weight (mg/g)	Liver weight (g)	Liver weight/body weight (mg/g)	Kidney weight (g)	Kidney weight/body weight (mg/g)	Plasma insulin (pmol/l)
FVB-starch	25.6±0.4	136±7	5.3±0.2	1.20±0.06	46.4±1.9	0.34±0.02	13.0±0.6	113.6±8.5
FVB-sucrose	26.3±0.6	137±6	5.2±0.2	1.21±0.05	46.2±1.5	0.35±0.01	13.5±0.5	244.7±14.0*
CAT-starch	25.6±0.5	141±8	5.5±0.3	1.26±0.02	49.1±0.7	0.37±0.03	14.3±0.9	108.1±8.3
CAT-sucrose	26.0±0.6	143±11	5.4±0.3	1.27±0.07	48.9±2.0	0.36±0.03	13.5±0.8	240.0±24.3*

Values are means±SEM, *n*=14 or 15 per group

**p*<0.05 vs corresponding starch group

detected between 480 and 520 nm. Qualitative changes in intracellular Ca^{2+} concentration were inferred from the ratio of the fura-2 fluorescence intensity (FFI) at two wavelengths. Fluorescence decay time was also measured as an indication of the intracellular Ca^{2+} clearing rate [21].

Protein carbonyl assay

Protein carbonyl content of total protein lysate was determined as described [22]. In brief, protein was precipitated by adding an equal volume of 20% trichloroacetic acid (TCA) and centrifuged (11,000 ×*g*) for 5 min. The sample was resuspended in 10 mmol/l 2,4-dinitrophenylhydrazine solution for 15–30 min at room temperature before 20% TCA was added and samples were centrifuged (11,000 *g*) for 3 min. The precipitate was resuspended in 6 mol/l guanidine solution. The maximum absorbance (360–390 nm) was read against appropriate blanks (2 mol/l HCl) and carbonyl content was calculated using the formula: absorption at 360 nm×45.45 nmol/protein content (mg).

Intracellular fluorescence measurement of ROS

Intracellular oxidant stress was monitored by changes in fluorescence intensity resulting from intracellular probe oxidation. Cardiomyocytes were loaded with 10 μmol/l 5-(6)-chloromethyl-2',7'-dichlorodihydrofluorescein diacetate (Molecular Probes, Eugene, OR, USA) for 30 min at 37°C before being washed with PBS buffer. Cells were sampled randomly using an Olympus BX-51 microscope equipped with an Olympus MagnaFire SP digital camera and ImagePro image analysis software (Media Cybernetics, Silver Spring, MD, USA). Fluorescence was calibrated with InSpeck microspheres (Molecular Probes). More than 150 cells per data point were evaluated using the grid-crossing method for cell selection in more than 20 visual fields [23].

Glucose-uptake measurement

Myocytes were cultured in a modified Dulbecco's modified Eagle's medium containing 5% FBS, 5.0 mmol/l glucose

and 1.0 mmol/l CaCl_2 at 37°C for 30 min. The cells were then washed three times with Krebs–Ringer–HEPES (KRH, 136 mmol/l NaCl, 4.7 mmol/l KCl, 1.25 mmol/l CaCl_2 , 1.25 mmol/l MgSO_4 , 10 mmol/l HEPES, pH 7.4) buffer and incubated with 2 ml KRH buffer at 37°C for 30 min. Some cells were exposed to insulin (100 nmol/l, 10 min). Glucose uptake was initiated by the addition of 0.1 ml KRH buffer and 2-deoxy-D- ^3H glucose (0.2 μCi/ml) and 5 mmol/l glucose. Glucose uptake was terminated 30 min later by washing the cells three times with cold PBS. The cells were lysed overnight with 0.5 ml 0.5 mol/l

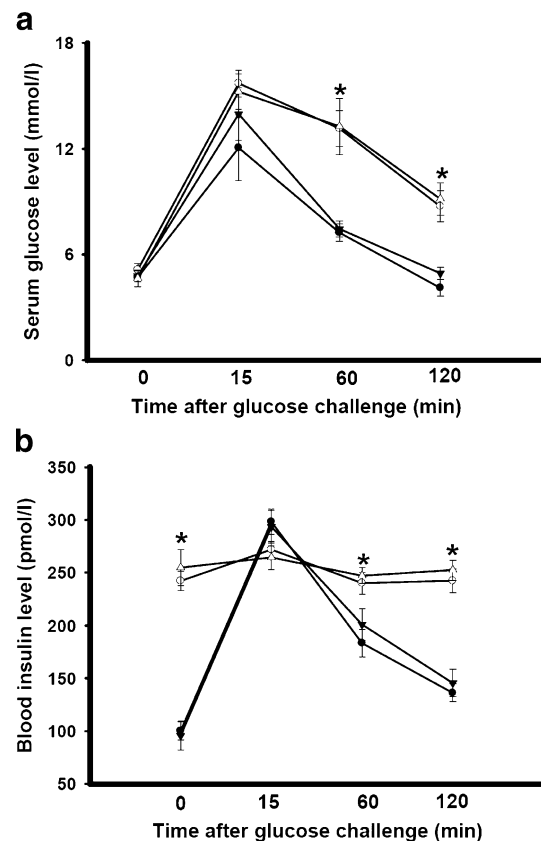


Fig. 1 Serum glucose (a) and blood insulin (b) levels in response to i.p. glucose challenge (2 g glucose/kg body weight) in starch- and sucrose-fed FVB and catalase (CAT) mice. Filled circles, FVB starch-fed; open circles, FVB sucrose-fed; filled triangles, CAT starch-fed; open triangles, CAT sucrose-fed. The mice were fasted for 12 h before the tests. Means±SEM, *n*=9 or 10 mice per group, **p*<0.05 between the starch- and sucrose-fed groups

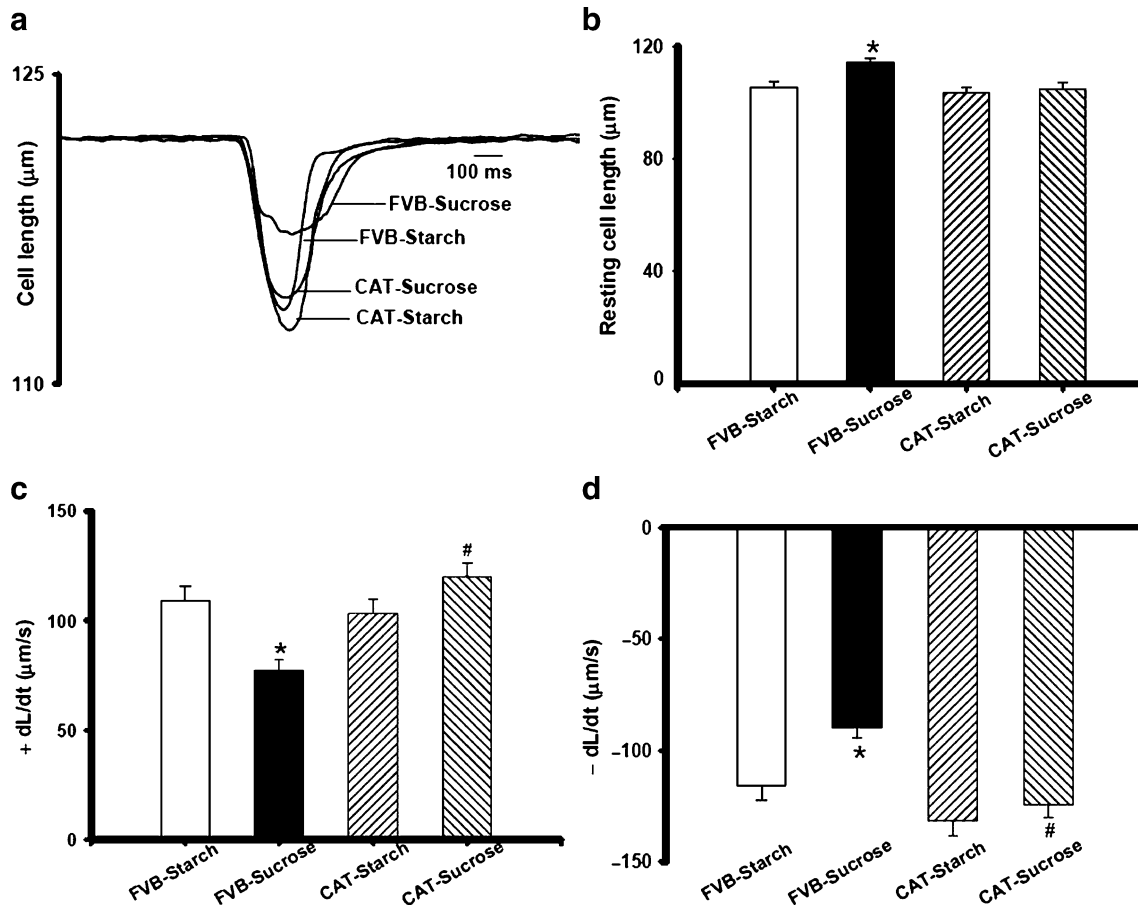


Fig. 2 Contractile properties of cardiomyocytes from starch- and sucrose-fed FVB and catalase (*CAT*) mouse hearts. **a** Representative traces depicting cell shortening in myocytes from each of the four groups; **b** resting cell length; **c** maximal velocity of shortening ($+dL/dt$);

and **d** maximal velocity of relengthening ($-dL/dt$). Means \pm SEM, $n=103$ – 135 cells/group, $*p<0.05$ vs FVB-starch group, $\#p<0.05$ vs FVB-sucrose group

NaOH and 0.1% SDS (w/v). The radioactivity retained by the cell lysates was determined by a scintillation counter (LC 6000IC; Beckmann, Fullerton, CA, USA) and normalised to the protein amount measured with a Bradford Protein Assay Kit [24, 25]. To minimise the inter-assay variation, glucose uptake in all cell groups was normalised to the corresponding FVB-starch group.

Western blot analysis of Akt, phosphorylated Akt (pAkt), eNOS, tyrosine phosphorylation of insulin receptor, PPAR γ , PTP1B, SERCA2a, NCX and PLB

Tissue or cardiomyocyte samples were homogenised, sonicated and centrifuged (12,000 g). Protein (50 μ g/lane) was separated on a Bio-Rad Minigel apparatus (Mini-PROTEAN II; Bio-Rad, Hercules, CA, USA) before being transferred to nitrocellulose membranes. Membranes were incubated for 1 h in a blocking solution containing 5% milk in Tris-buffered saline (TBS), then were washed in TBS and incubated overnight at 4°C with anti-Akt (1:1,000),

anti-pAkt (1:1,000), anti-PTP1B (1:2,500), anti-SERCA2a (1:1,000), anti-NCX (1:1,000), anti-PLB (1:1,000), anti-tyrosine phosphorylation of insulin receptor (1:1,000) and anti-PPAR γ (1:1,000) antibodies. Anti-Akt, anti-pAkt (Ser473), anti-PPAR γ and anti-tyrosine phosphorylation of insulin receptor (Tyr1146) antibodies were obtained from Cell Signaling (Beverly, MA, USA). PTP1B antibody was from BD Biosciences Pharmingen (San Diego, CA, USA), antibodies to SERCA2a (A7R5) and PLB (2D12) were kindly provided by S. Cala (Wayne State University, Detroit, MI, USA). Anti-NCX antibodies were obtained from Swant Company (Bellinzona, Switzerland). After removal of excess primary antibody binding, blots were incubated for 1 h with horseradish peroxidase-conjugated secondary antibody. Antibody binding was detected using enhanced chemiluminescence and films were evaluated with a Bio-Rad Calibrated Densitometer [21].

Data analysis

Data are expressed as means \pm SEM. Statistical comparisons were performed by ANOVA followed by a Newman–Keuls post hoc test. Significance was defined as $p<0.05$.

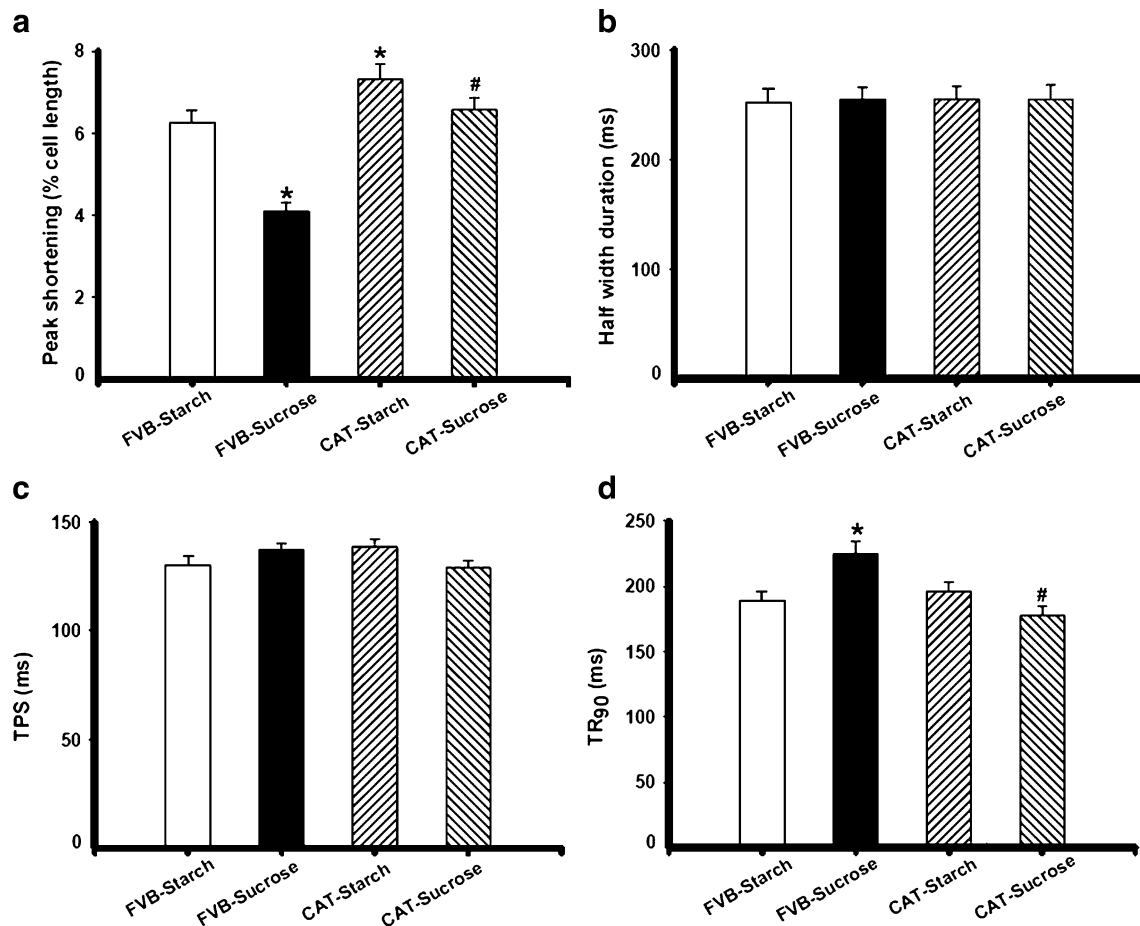


Fig. 3 Contractile properties of cardiomyocytes from starch- and sucrose-fed FVB and catalase (*CAT*) mouse hearts. **a** Peak shortening (normalised to cell length); **b** half-width duration; **c** time-to-peak shortening (*TPS*); and **d** time-to-90% relengthening (*TR₉₀*). Means±SEM, *n*=103–135 cells/group, *HDI60230<0.05 vs FVB-starch group, #*p*<0.05 vs FVB-sucrose group

Results

Experimental animals

No significant difference was found in body, heart, liver and kidney weight or organ/body weight ratio among all mouse groups. Consistent with the previous findings [5, 6, 19], sucrose induced hyperinsulinaemia, which was not affected by the catalase transgene (Table 1). Following acute i.p. glucose challenge, blood glucose and insulin levels in starch-fed mice started to drop after peaking at 15 min, and returned to nearly baseline values after 120 min. However, the post-challenge glucose levels were maintained at high levels from 15 to 120 min in the sucrose-fed mice. Similarly, basal blood insulin levels were significantly higher in sucrose-fed FVB or catalase mice, and were barely responsive to acute i.p. glucose challenge (Fig. 1). The blood insulin levels were significantly higher in sucrose-fed mice than those of starch-fed mice at every time-point except 15 min. These data revealed impaired glucose clearance and insulin insensitivity following sucrose feeding. There was no difference in basal fasting glucose levels among all mouse groups, excluding the presence of diabetes following sucrose dietary intake.

Mechanical and fluorescent properties of myocytes from starch- and sucrose-fed mice

The 12-week sucrose feeding regimen significantly enhanced the resting cell length of cardiac myocytes, which may be ablated by catalase transgene. Catalase itself did not affect the resting cell length (Fig. 2). As shown in Figs. 2 and 3, PS and $\pm dL/dt$ were significantly depressed in myocytes from the sucrose-fed FVB group compared with those from starch-fed FVB mice. Myocytes from sucrose-fed FVB mice displayed normal TPS and a significantly prolonged *TR₉₀* compared with those from the starch-fed FVB mice. The HWD, an index of the duration of late-contraction and early-relaxation, did not differ among all mouse groups. Interestingly, catalase effectively protected cardiomyocytes from sucrose-diet-induced mechanical dysfunctions. Our fura-2 study revealed depressed electrically stimulated ΔFFI and slowed intracellular Ca^{2+} clearing rate in myocytes from sucrose-fed FVB myocytes, a finding consistent with reduced PS and prolonged *TR₉₀* in these myocytes. Similarly to its effect on cell shortening, catalase abolished the sucrose-diet-induced decrease in ΔFFI and prolongation in intracellular Ca^{2+} clearing. The resting intracellular

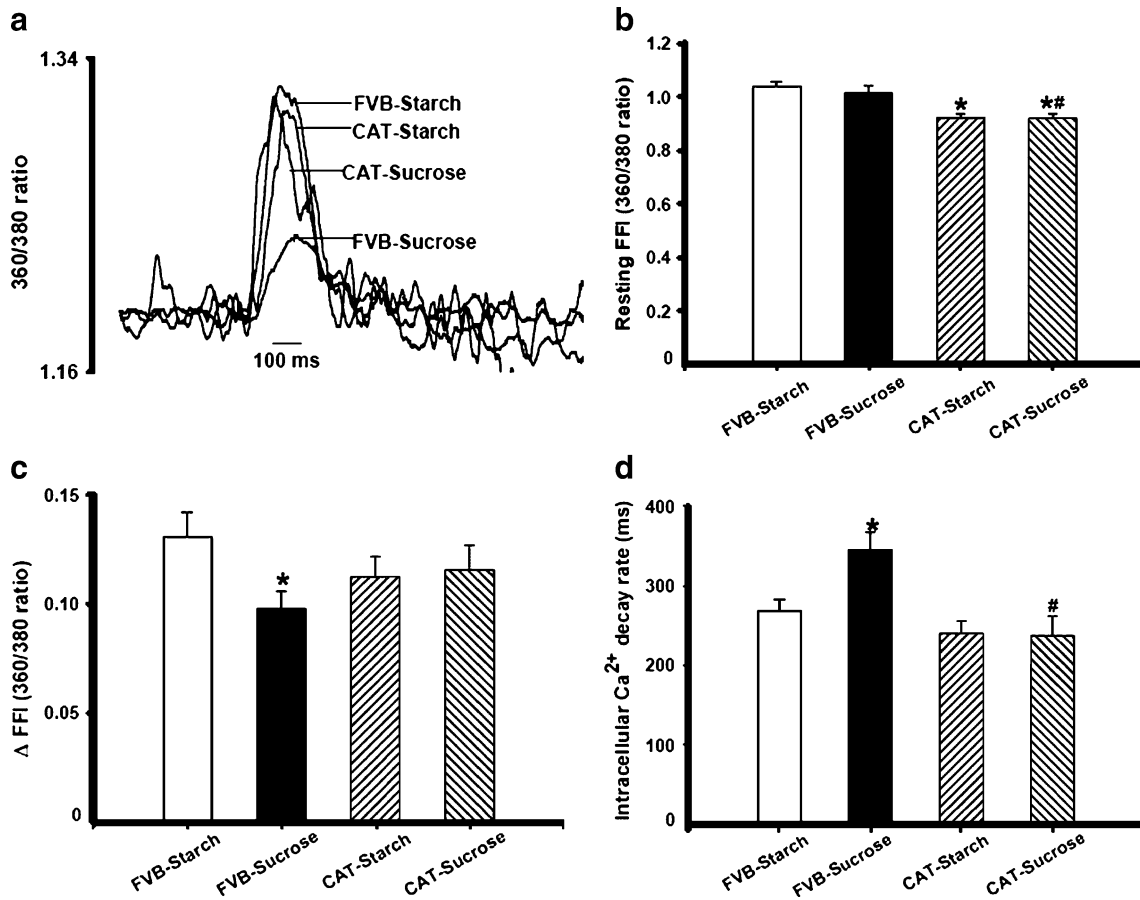


Fig. 4 Intracellular Ca²⁺ transient properties in cardiomyocytes from starch- and sucrose-fed FVB and catalase (CAT) mouse hearts. **a** Representative traces depicting intracellular Ca²⁺ transients in myocytes from each of the four groups; **b** resting intracellular Ca²⁺

fura-2 fluorescence intensity (FFI); **c** electrically stimulated increase in FFI (ΔFFI); and **d** intracellular Ca²⁺ transient decay rate. Means±SEM, n=31–43 cells/group, *p<0.05 vs FVB-starch group, #p<0.05 vs FVB-sucrose group

Ca²⁺ levels (resting FFI) were unaltered by sucrose diet although they were significantly reduced by catalase (Fig. 4).

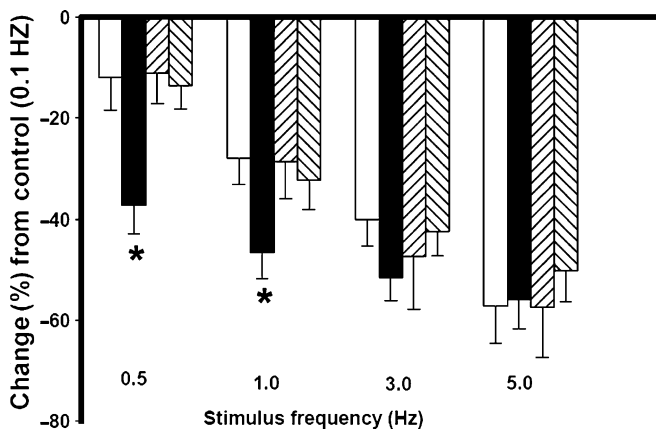


Fig. 5 Peak shortening amplitude of ventricular myocytes from starch- and sucrose-fed FVB and catalase (CAT) mouse hearts at different stimulus frequencies (0.1, 0.5, 1.0, 3.0 and 5.0 Hz). PS at each stimulus frequency was normalised to that of 0.1 Hz of the same cell. *Open bars*, FVB starch fed; *filled bars*, FVB sucrose fed; *hatched (rising left to right) bars*, CAT starch-fed; *hatched (rising right to left) bars*, CAT sucrose fed. Means±SEM, n=20 cells per animal group. *p<0.05 vs starch-fed FVB group

Effect of increasing stimulation frequency on myocyte shortening

Rodent hearts normally contract at high frequencies, whereas our mechanical evaluation was conducted at 0.5 Hz. To evaluate the impact of insulin resistance and catalase on cardiac contractile function under higher frequencies, we increased the stimulating frequency up to 5.0 Hz (300 beats/min). Cells were initially stimulated to contract at 0.5 Hz for 5 min to ensure a steady-state before commencing the frequency study. All recorded PSs were normalised to that obtained at 0.1 Hz in the same myocyte. Figure 5 shows a steeper inhibition in PS from sucrose-fed FVB mouse myocytes at 0.5 and 1.0 Hz of stimulating frequency compared with the starch-fed FVB group, suggesting that intracellular Ca²⁺ cycling function may be compromised under insulin resistance. However, the degree of PS reduction was similar between starch- and sucrose-fed groups at 3.0 and 5.0 Hz, indicating normal

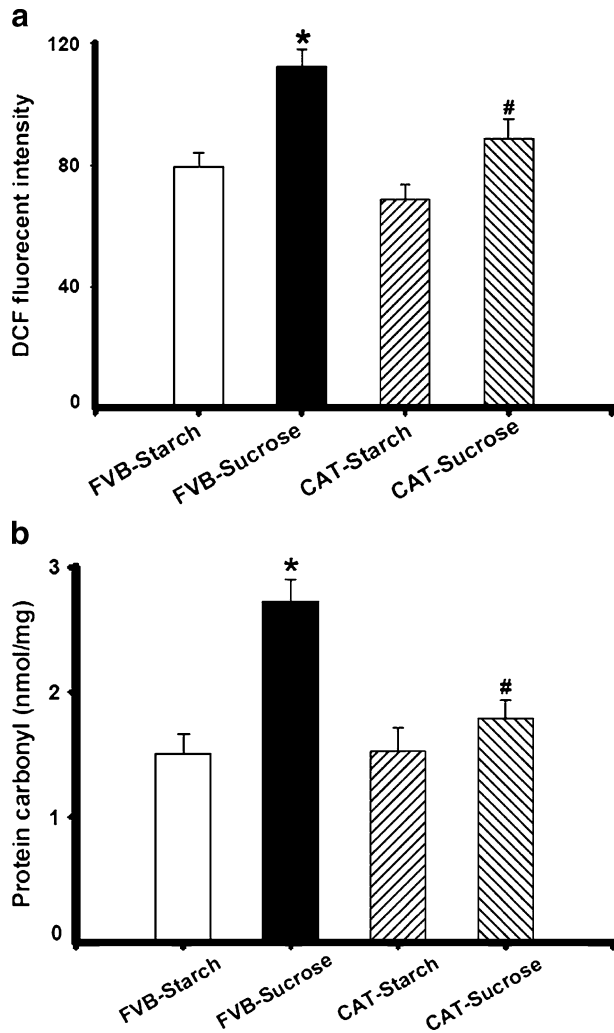


Fig. 6 Levels of cardiac ROS generation (a) and protein carbonyl formation (b) from FVB and catalase (*CAT*) mice fed with either starch or sucrose diet for 12 weeks. Means \pm SEM, $n=20$ and 6 for ROS and protein carbonyl formation, respectively, * $p<0.05$ vs FVB-starch group, # $p<0.05$ vs FVB-sucrose group. DCF 5-(6)-chloromethyl-2',7'-dichlorodihydrofluorescein diacetate

Ca²⁺ recycling capacity under insulin resistance at these frequencies. Interestingly, catalase nullified sucrose-diet-induced augmentation in inhibition of PS at 0.5 and 1.0 Hz while it elicited little effect on the stimulus frequency–PS relationship.

Effect of sucrose diet and catalase transgene on ROS and protein carbonyl formation

Results shown in Fig. 6 indicate that ROS generation and protein carbonyl formation, an indicator of protein oxidative damage, were significantly elevated in myocardium from sucrose-fed FVB mice. Although catalase itself had no effect on cardiac ROS generation and protein carbonyl formation, it significantly attenuated sucrose-diet-induced elevation in cardiac ROS generation and protein carbonyl formation, suggesting enhanced cardiac ROS accumulation

and protein oxidative damage under insulin resistance and protection offered by the antioxidant catalase.

Effect of sucrose diet and catalase transgene on insulin-stimulated glucose uptake

To determine whether insulin sensitivity plays a role in sucrose-diet- and catalase-induced alteration of cardiomyocyte contractile function, basal and insulin-stimulated glucose uptake was determined. Basal glucose uptake was comparable in all groups. At 100 nmol/l insulin, starch-fed FVB mouse myocytes exhibited a significant increase in glucose uptake. However, the insulin-stimulated glucose uptake was blunted in myocytes from sucrose-fed FVB mice compared with the starch-fed FVB group. Catalase elicited little effect on insulin-stimulated glucose uptake in either starch- or sucrose-fed mouse myocytes. Insulin-stimulated glucose uptake remained blunted in the sucrose-fed catalase group (Fig. 7). These data suggest that catalase transgene does not affect insulin-stimulated glucose uptake in either starch- or sucrose-fed mouse cardiomyocytes.

Changes of protein expression in SERCA2a, PLB and NCX

To examine the possible mechanism behind insulin-resistance-induced cardiomyocyte contractile dysfunction and catalase-elicited protection, we evaluated cardiac expression of several key cardiac Ca²⁺-regulating proteins including SERCA2a, PLB and NCX. Our results revealed that sucrose diet did not significantly affect expression of SERCA2a and PLB, although it downregulated NCX

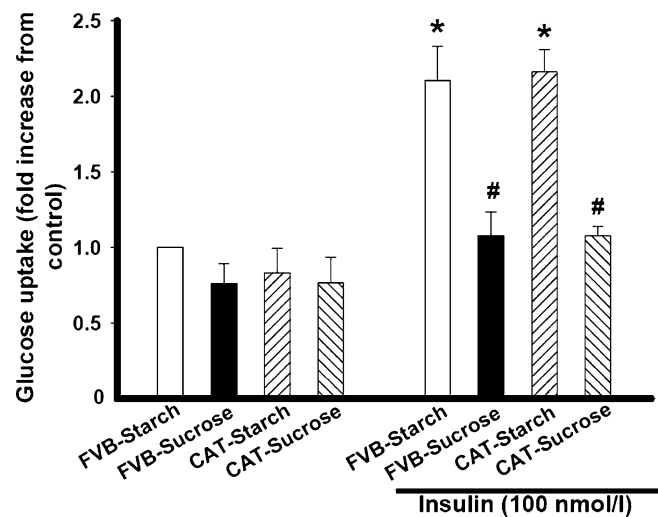


Fig. 7 Basal and insulin (100 nmol/l)-stimulated 2-deoxy-D-[³H] glucose uptake in myocytes from starch- and sucrose-fed FVB and catalase (*CAT*) mouse hearts. All measurements are shown as fold increase of the respective control (FVB-Starch) value from the same assay. Means \pm SEM, $n=3$ or 4 preparations per group, * $p<0.05$ vs the respective group without insulin challenge, # $p<0.05$ vs corresponding starch diet group

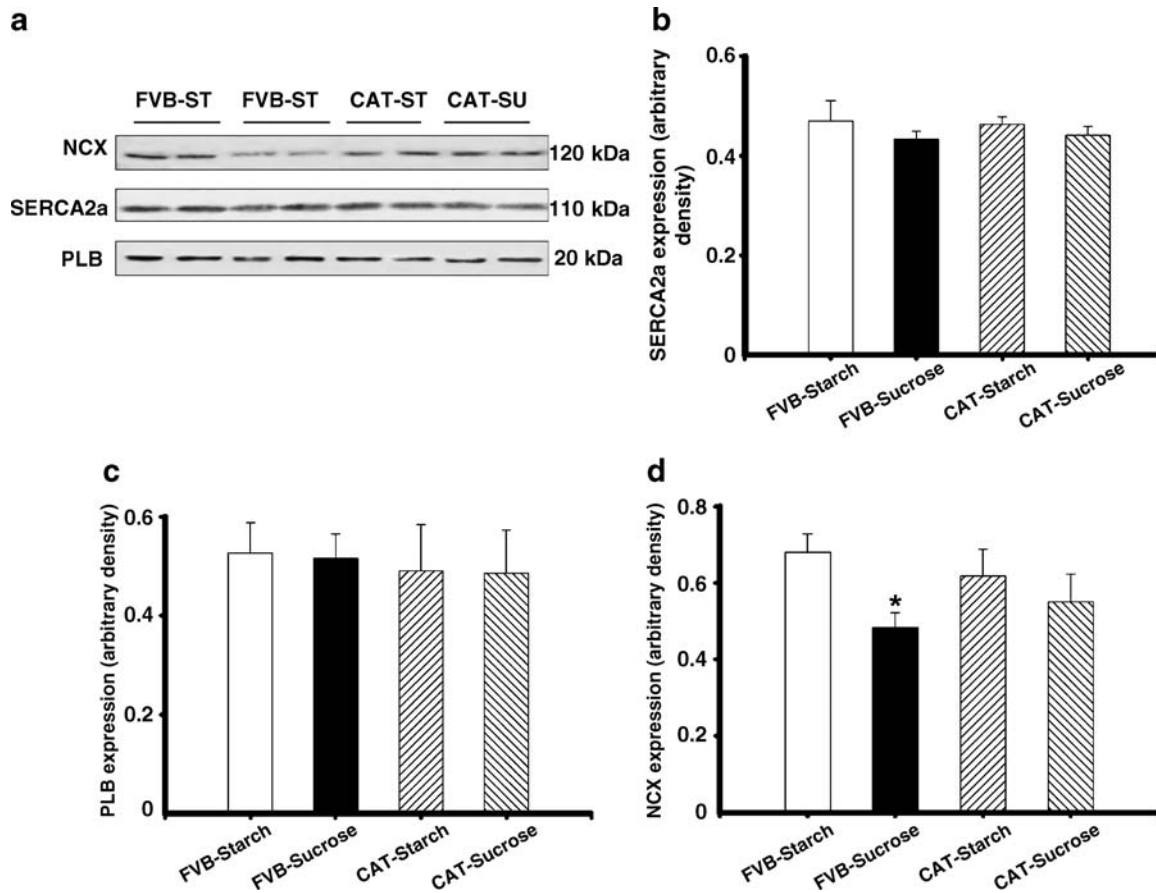


Fig. 8 Western blot analysis showing SERCA2a, PLB and NCX expression in starch- (ST) and sucrose (SU)-fed FVB and catalase (CAT) mouse hearts. **a** Representative immunoblots depicting SERCA2a, PLB and NCX expression using anti-SERCA2a, anti-PLB and anti-NCX antibodies; **b** SERCA2a expression; **c** PLB expression; and **d** NCX expression. Means \pm SEM, $n=4$, * $p<0.05$ vs FVB-starch group

expression. Interestingly, sucrose-diet-induced downregulation of NCX was absent in catalase-transgenic mice (Fig. 8), suggesting a role of NCX in sucrose-diet-induced mechanical dysfunction and in the cardiac protective effect elicited by catalase.

Changes of protein expression in Akt, pAkt, tyrosine phosphorylation of insulin receptor, PPAR γ PTP1B and eNOS

Insulin resistance is associated with interrupted insulin signalling at receptor and post-receptor levels [1, 3]. To explore the contribution of insulin-signalling molecules to catalase-afforded cardiac protection against insulin-resistance-elicited mechanical dysfunction, we evaluated cardiac expression of Akt, pAkt, tyrosine phosphorylation (site Tyr1146) of the insulin receptor, PPAR γ , PTP1B and eNOS. Our results showed that sucrose-feeding-induced insulin resistance did not affect expression of total Akt with or without insulin stimulation. However, sucrose diet significantly enhanced basal Akt phosphorylation and blunted insulin-stimulated Akt phosphorylation. Catalase did not affect sucrose-diet- or insulin-stimulation-induced

effects on Akt and pAkt (Fig. 9). Our further study revealed that insulin resistance significantly enhanced expression of PTP1B without affecting that of PPAR γ and basal tyrosine phosphorylation of insulin receptor. The insulin-resistance-induced rise in PTP1B level was further augmented by the catalase transgene. Catalase also upregulated expression of PTP1B and PPAR γ but not insulin-receptor tyrosine phosphorylation (basal or insulin-stimulated). Consistent with its effect on Akt phosphorylation shown in Fig. 9, insulin-stimulated phosphorylation of insulin receptor was significantly inhibited by sucrose feeding. Catalase itself did not affect insulin-stimulated insulin-receptor phosphorylation. These data did not favour a likely contribution of insulin-receptor signalling to catalase-elicited cardiac protection against insulin resistance. Interestingly, insulin resistance induced a significant decrease in eNOS expression, which was blunted by catalase transgene (Fig. 10).

Discussion

Our results revealed that prediabetic insulin resistance elicits hyperinsulinaemia, glucose intolerance, impaired insulin-stimulated glucose uptake, cardiomyocyte contrac-

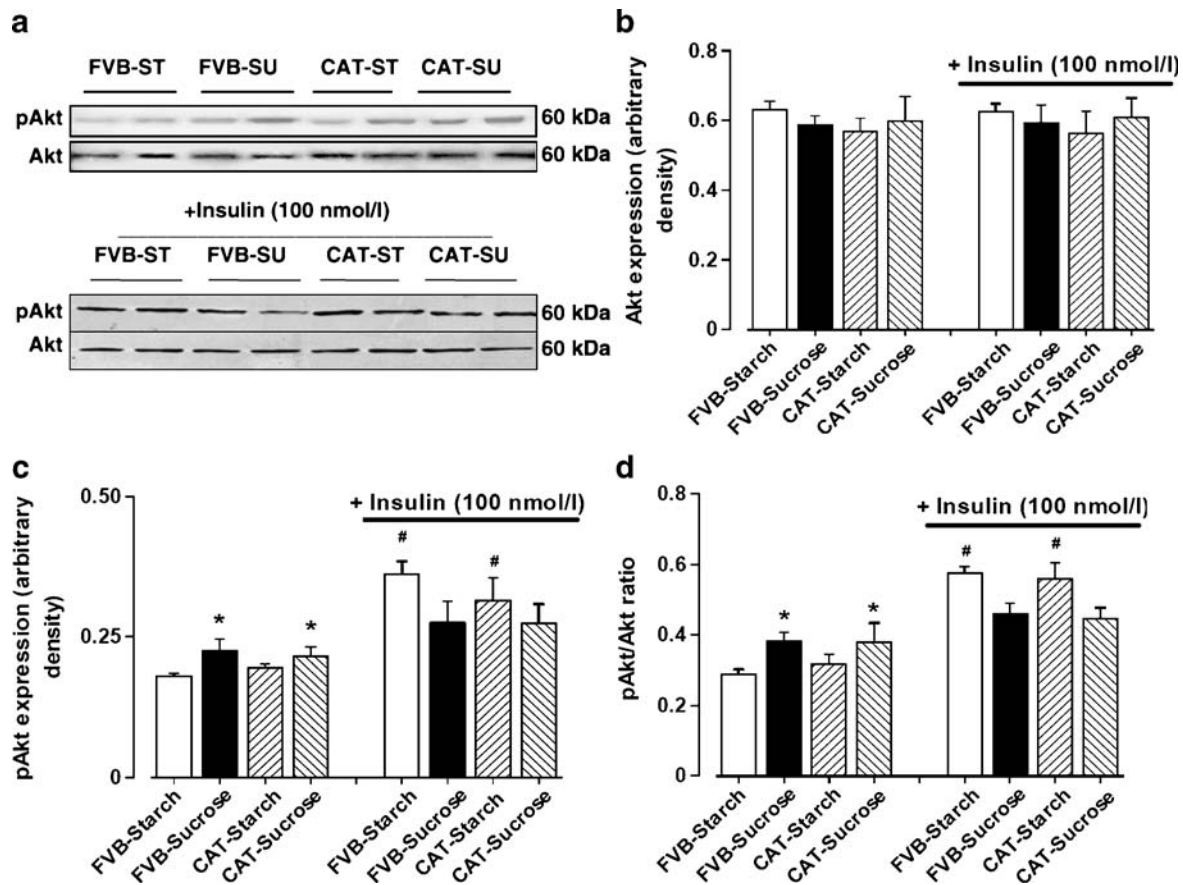


Fig. 9 Western blot analysis showing total and phosphorylated Akt level in starch- (ST) and sucrose (SU)-fed FVB and catalase (CAT) mouse cardiomyocytes challenged with or without insulin (100 nmol/l for 10 min). **a** Representative immunoblots depicting total and phosphorylated Akt using anti-Akt and anti-phospho-Akt

(pAkt) antibodies. **b** Total Akt expression; **c** pAkt expression; and **d** pAkt/Akt ratio. Means \pm SEM, $n=8$ and 4 for non-insulin- and insulin-stimulated groups, respectively, * $p<0.05$ vs FVB-starch group, # $p<0.05$ vs corresponding non-insulin-stimulated group

tile dysfunction, impaired intracellular Ca^{2+} handling and enhanced ROS generation and protein damage, as well as reduced NCX expression. With the exception of hyperinsulinaemia, glucose intolerance and impaired insulin-stimulated glucose uptake, all of the above were alleviated by catalase. The 'sucrose diet' insulin-resistance-induced cardiac contractile and intracellular Ca^{2+} dysfunctions were associated with enhanced basal Akt phosphorylation and PTP1B expression, blunted insulin stimulation in phosphorylation of Akt and insulin receptor (Tyr1146) and reduced expression of eNOS but not that of PPAR γ or basal insulin-receptor tyrosine phosphorylation, which suggests a relationship between altered insulin signalling and cardiac mechanical dysfunction. However, unlike its beneficial effect on insulin-resistance-induced mechanical and intracellular Ca^{2+} dysfunction, catalase failed to alleviate the insulin-resistance-induced deficiency in insulin sensitivity and post-receptor signalling. Only reduced expression of eNOS in response to insulin resistance, which may or may not be directly associated with the insulin-signalling pathway, was alleviated by catalase. Given the fact that whole-body insulin resistance, hyperinsulinaemia, impaired glucose uptake and glucose intolerance were unaffected by catalase, our data indicated that

catalase rescues insulin-resistance-induced cardiac contractile dysfunction possibly through reduction of ROS generation and protein oxidation as well as restoration of NCX expression, a mechanism independent of insulin signalling.

Insulin resistance impairs cardiac contractile functions in a manner reminiscent of full-blown diabetes [9, 10], suggesting a possible role of prediabetic insulin resistance in diabetic cardiomyopathy. This is supported by the beneficial effects of pharmacological intervention and lifestyle modification including insulin sensitiser, diet restriction and weight loss on insulin sensitivity and cardiac function in patients with type 2 diabetes and obesity [3, 25]. Our 12-week starch/sucrose dietary feeding did not produce any difference in body or organ weight and fasting blood glucose in either FVB or catalase mice, excluding the potential contribution of obesity and diabetes to the current insulin-resistance experimental model. Data from our present study revealed that ventricular myocytes from sucrose-fed mice exhibited depressed PS amplitude, reduced $\pm dL/dt$ and prolonged TR_{90} associated with normal TPS and HWD. Most of these data are consistent with our previous findings using a similar hyperinsulinaemic insulin-resistance model in rats [6, 26]. The fact that

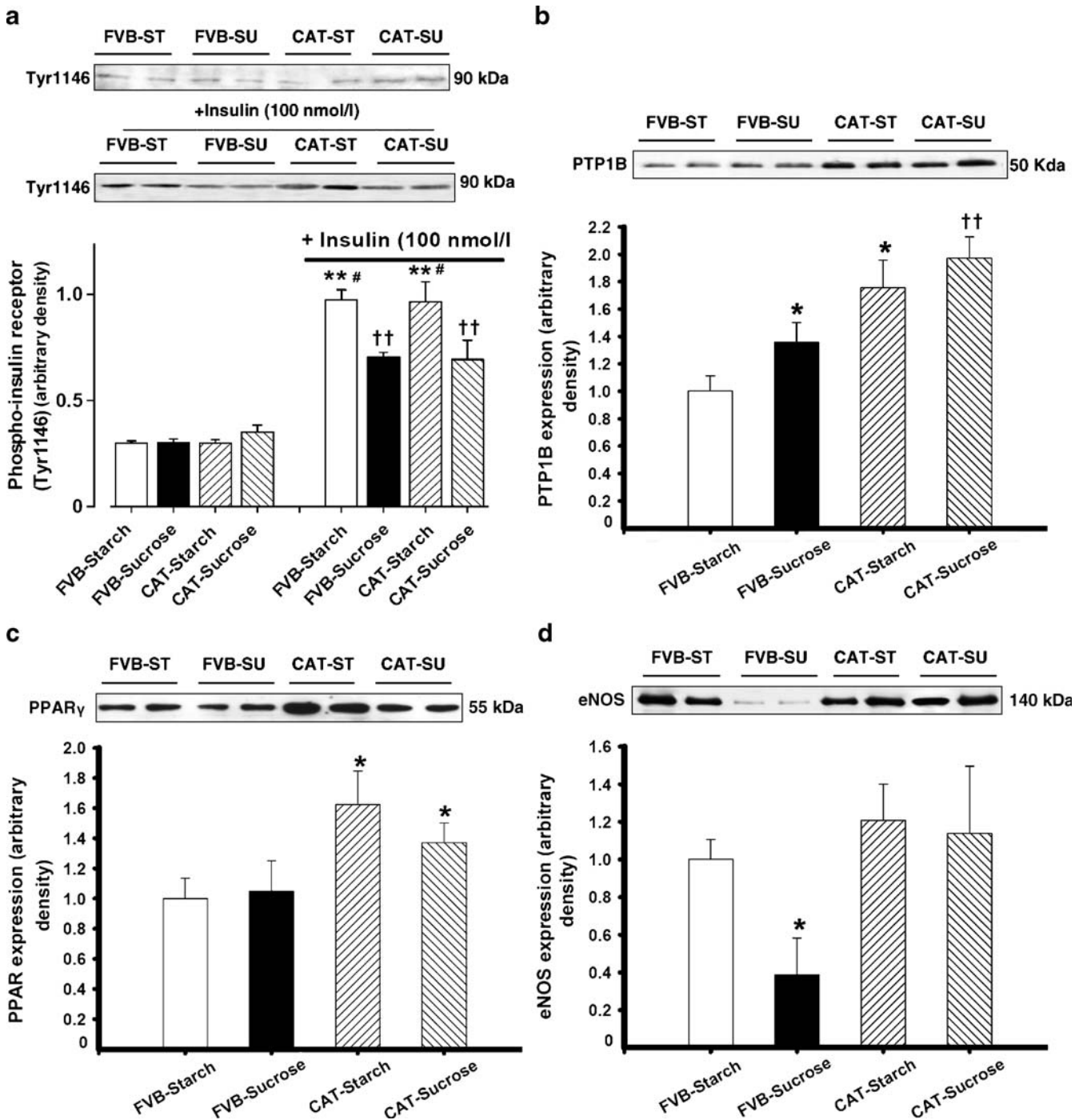


Fig. 10 Western blot analysis showing expression of insulin-receptor phosphorylation (a), PTP1B (b), PPAR γ (c) and eNOS (d) in starch (ST) and sucrose (SU)-fed FVB and catalase (CAT) mouse hearts. For insulin-receptor phosphorylation (Tyr1146), cardiomyocytes from each of the four groups were treated with or without insulin (100 nmol/l) for 10 min. Insets: Representative immunoblots depicting

phosphorylation of insulin receptor, PTP1B, PPAR γ and eNOS using anti-phospho-insulin receptor (Tyr1146), anti-PTP1B, anti-PPAR γ and anti-eNOS antibodies. Means \pm SEM, $n=8$ and 4 for non-insulin and insulin-stimulated groups, respectively, * $p<0.05$ vs FVB-starch group, †* $p<0.05$ vs corresponding non-insulin-stimulated group, # $p<0.05$ vs FVB-sucrose or corresponding sucrose diet group

our early observation showed either normal TR₉₀ and \pm dL/dt or shortened TPS after sucrose-diet feeding may be attributed to relatively short feeding duration (7–10 weeks) [6] and the difference in experimental species (rats vs mice). These mechanical defects are strikingly similar to those reported in ventricular myocytes from full-blown

diabetes [9, 18, 26]. The increased resting cell length in conjunction with unchanged heart weight or heart:body weight ratio in sucrose-fed mice suggests the possible existence of dilated cardiomyopathy or ‘eccentric cardiac hypertrophy’ due to volume-overload-induced stretch of ventricles. Insulin resistance is known to be accompanied

by ventricular pressure or volume overload [2]. The impaired intracellular Ca^{2+} handling shown as a reduced intracellular Ca^{2+} clearance rate (τ) and reduced ΔFFI in sucrose-fed FVB mouse myocytes are consistent with those found in diabetic hearts [9, 10, 18] and are mostly likely responsible for prolonged TR_{90} and reduced PS amplitude in these cells. The unchanged HWD in conjunction with prolonged relaxation duration and normal contraction duration following sucrose feeding favours the view that impaired relaxation may be due to a defect of the slow phase of relaxation (controlled by NCX and/or the sarcolemmal Ca^{2+} pump) rather than early relaxation machinery such as myosin heavy chain isozymes and SERCA. This is consistent with our immunoblotting of reduced NCX expression associated with normal SERCA2a and PLB in the sucrose-fed FVB group. The observation that the catalase transgene itself significantly lowered the resting intracellular Ca^{2+} level may indicate possible protective effects of the antioxidant enzyme against intracellular Ca^{2+} overload in the heart. H_2O_2 , the substrate of the catalase enzymatic reaction, is known to lead to accumulation of intracellular Ca^{2+} and Ca^{2+} overload in cardiac myocytes [27].

Perhaps the most intriguing finding from our study was that catalase elicits cardiac protection against insulin resistance independently of an improvement in insulin sensitivity. The mechanical and intracellular Ca^{2+} defects triggered by insulin resistance were alleviated by catalase, in a manner similar to its effect on diabetes-induced cardiac contractile dysfunctions [18]. Cardiomyocyte dysfunction has been demonstrated in animal models of type 2 diabetes or insulin resistance [4–6, 26, 28, 29]. It could be speculated that reduced oxidative stress is responsible for the protection by catalase against insulin-resistance-induced cardiac contractile dysfunction. This is evidenced by the antagonism of catalase against the insulin-resistance-induced increase in cardiac ROS generation and protein carbonyl formation. Another scenario behind catalase-elicited protection against insulin-resistance-associated cardiomyocyte dysfunction is the antagonism against depressed NCX expression. NCX is an essential cardiac Ca^{2+} -regulating protein responsible for cardiac contractile function, especially the delayed phase of relaxation [30]. SERCA2a and PLB also play major roles in the maintenance of cardiac contractile function, especially the rapid phase of relaxation [31]. Nevertheless, our current finding does not favour any involvement of SERCA2a and PLB in insulin resistance or the catalase-elicited cardiac mechanical effect. Although our study revealed changes of several insulin-signalling molecules in insulin-resistant FVB mice, at both the receptor and post-receptor levels, improvement of cardiac ROS production, protein carbonyl formation and NCX expression in sucrose-fed catalase mice seem to occur independently of these insulin-signalling molecules (tyrosine phosphorylation of insulin receptor, Akt phosphorylation, PTP1B and PPAR γ). This separation between contractile function and insulin signalling was further supported by the inability of catalase transgene to correct insulin-resistance-dampened glucose uptake.

Our data do not favour an involvement of the insulin-signalling cascade in the catalase-elicited protection of cardiomyocyte dysfunction. Nevertheless, several interesting points may be helpful to better understand insulin-signalling mechanisms in cardiomyocytes. Our observation of normal tyrosine phosphorylation of the insulin receptor and enhanced Akt phosphorylation in insulin-resistant mice may indicate a ‘pseudo-hyperactivity’ of insulin signalling due to a feedback upregulation as a result of desensitised insulin signalling following 12 weeks of sucrose feeding. Either under- or overactivation of the key cardiac survival factor Akt has been demonstrated in various models of type 2 diabetes or insulin resistance [32–34], suggesting a crucial role of Akt activation in insulin resistance. It is noteworthy that enhanced Akt phosphorylation may also be attributed to elevated blood insulin levels in sucrose-fed mice. It is not surprising that sucrose-feeding-induced insulin resistance upregulated PTP1B, the negative modulator of insulin signalling [15]. Protein-tyrosine phosphatases (PTPs) are extremely sensitive to oxidative stress, which has been suggested as a mechanism for regulation of PTP function [35]. Although oxidative stress may facilitate the tyrosine-phosphorylation-dependent cellular-signalling response of insulin by transiently inactivating the negative-insulin-regulator PTPs, excessive oxidative stress under insulin resistance and diabetes was reported to upregulate the redox-sensitive protein PTP1B [36]. Reduced oxidative stress along with elevated PTP1B expression in sucrose-fed catalase mice again proved the independence of oxidative stress and insulin signalling in our current model of insulin resistance. Furthermore, PPAR γ is the adipocyte-predominant transcription factor serving as an insulin sensitiser for glucose and lipid metabolism [14]. Although sucrose-fed insulin resistance failed to alter PPAR γ in our current experimental setting, the fact that catalase transgene itself directly enhanced PPAR γ levels should assist in correcting the imbalanced redox status triggered by insulin resistance.

Our results indicate that insulin resistance reduced the expression of eNOS, which can be alleviated by the antioxidant catalase. It has been reported previously that reduced eNOS function may underscore cardiac and smooth muscle atherogenesis in fructose-induced insulin resistance and metabolic syndrome [37]. Recent evidence from our laboratory revealed that gene delivery of eNOS into cardiomyocytes directly improved cardiac contractile function through a phosphatidylinositol-3-kinase-dependent mechanism [35]. Additional evidence suggested that impairment of endothelium-dependent vasodilatation is not a direct consequence of reduced activity/expression of eNOS, but is rather triggered by an enhanced inactivation of nitric oxide by oxidative stress, especially ROS [38]. Oxidative stress and impaired cardiac contractile function have been demonstrated in insulin-resistant states such as type 2 diabetes, hypertension and obesity [1, 39]. A high-fructose diet has been shown to reduce mRNA expression of antioxidant catalase [40], which itself provides solid support for a therapeutic indication of catalase enzyme. Our present study indicates that the catalase-elicited

cardiac-protective effect on mechanical function may be related solely to its antioxidant capacity, independently of improved insulin sensitivity. This is somewhat inconsistent with an earlier report that abrogation of oxidative stress improves insulin sensitivity in a Ren2 angiotensin-II-overexpression rat model [41]. It could be argued that catalase-induced upregulation of PPAR γ non-specifically improves cardiac function. Further study is warranted to elucidate the role of PPAR γ activation in cardiac contractile function and oxidative stress.

In summary, our present study sheds some light on the interactions between oxidative stress, insulin signalling and insulin-resistance-associated cardiac contractile defects. Given the fact that the precise pathogenesis of cardiac contractile dysfunction, cardiac Ca²⁺-regulatory protein defect and protein oxidative damage under insulin resistance is far from clear, it is imperative for researchers to delineate the action of insulin-signalling mechanisms under various conditions of oxidative stress in order to better understand the transition from insulin sensitive- to insulin-resistant states.

Acknowledgements This work was supported in part by the American Heart Association Northland Affiliate (#9960204Z) and Pacific Mountain Affiliate (#0355521Z) and American Diabetes Association (7-0-RA-21) to J. Ren. The catalase founder mice were kindly provided by P. N. Epstein from University of Louisville, Louisville, KY, USA. The anti-PLB antibody was kindly provided by S. Cala, Wayne State University, Detroit, MI, USA. Technical assistance from B. H. Zhao and J. Sotillo was greatly appreciated. Part of this work was presented at the 12th World Congress on Heart Disease in Vancouver, British Columbia, Canada, 16–19 July, 2005.

References

- Ceriello A, Motz E (2004) Is oxidative stress the pathogenic mechanism underlying insulin resistance, diabetes, and cardiovascular disease? The common soil hypothesis revisited. *Arterioscler Thromb Vasc Biol* 24:816–823
- Reaven GM (1995) Pathophysiology of insulin resistance in human disease. *Physiol Rev* 75:473–486
- Wang CC, Goalstone ML, Draznin B (2004) Molecular mechanisms of insulin resistance that impact cardiovascular biology. *Diabetes* 53:2735–2740
- Davidoff AJ, Mason MM, Davidson MB et al (2004) Sucrose-induced cardiomyocyte dysfunction is both preventable and reversible with clinically relevant treatments. *Am J Physiol Endocrinol Metab* 286:E718–E724
- Dutta K, Podolin DA, Davidson MB, Davidoff AJ (2001) Cardiomyocyte dysfunction in sucrose-fed rats is associated with insulin resistance. *Diabetes* 50:1186–1192
- Hintz KK, Aberle NS II, Ren J (2003) Insulin resistance induces hyperleptinemia, cardiac contractile dysfunction but not cardiac leptin resistance in ventricular myocytes. *Int J Obes Relat Metab Disord* 27:1196–1203
- Mazumder PK, O'Neill BT, Roberts MW et al (2004) Impaired cardiac efficiency and increased fatty acid oxidation in insulin-resistant ob/ob mouse hearts. *Diabetes* 53:2366–2374
- Gargiulo P, Jacobellis G, Vaccari V, Andreani D (1998) Diabetic cardiomyopathy: pathophysiological and clinical aspects. *Diab Nutr Metab* 11:336–346
- Ren J, Davidoff AJ (1997) Diabetes rapidly induces contractile dysfunctions in isolated ventricular myocytes. *Am J Physiol Heart Circ Physiol* 272:H148–H158
- Ren J, Ceylan-Isik AF (2004) Diabetic cardiomyopathy: do women differ from men. *Endocrine* 25:73–84
- Cusi K, Maezono K, Osman A et al (2000) Insulin resistance differentially affects the PI 3-kinase- and MAP kinase-mediated signaling in human muscle. *J Clin Invest* 105:311–320
- Dorrestijn J, Ouwens DM, Van den Berghe N, Bos JL, Maassen JA (1996) Expression of a dominant-negative Ras mutant does not affect stimulation of glucose uptake and glycogen synthesis by insulin. *Diabetologia* 39:558–563
- Hinault C, Mothe-Satney I, Gautier N, Lawrence JC Jr, Van Obberghen E (2004) Amino acids and leucine allow insulin activation of the PKB/mTOR pathway in normal adipocytes treated with wortmannin and in adipocytes from db/db mice. *FASEB J* 18:1894–1896
- Rangwala SM, Lazar MA (2004) Peroxisome proliferator-activated receptor gamma in diabetes and metabolism. *Trends Pharmacol Sci* 25:331–336
- Zabolotny JM, Haj FG, Kim YB et al (2004) Transgenic overexpression of protein-tyrosine phosphatase 1B in muscle causes insulin resistance, but overexpression with leukocyte antigen-related phosphatase does not additively impair insulin action. *J Biol Chem* 279:24844–24851
- Fisher TL, White MF (2004) Signaling pathways: the benefits of good communication. *Curr Biol* 14:R1005–R1007
- Cai L, Kang YJ (2001) Oxidative stress and diabetic cardiomyopathy: a brief review. *Cardiovasc Toxicol* 1:181–193
- Ye G, Metreveli NS, Donthi RV et al (2004) Catalase protects cardiomyocyte function in models of type 1 and type 2 diabetes. *Diabetes* 53:1336–1343
- Podolin DA, Sutherland E, Iwahashi M, Simon FR, Pagliassotti MJ (1998) A high-sucrose diet alters the lipid composition and fluidity of liver sinusoidal membranes. *Horm Metab Res* 30:195–199
- Kang YJ, Chen Y, Epstein PN (1996) Suppression of doxorubicin cardiotoxicity by overexpression of catalase in the heart of transgenic mice. *J Biol Chem* 271:12610–12616
- Zhang X, Klein AL, Alberle NS et al (2003) Cardiac-specific overexpression of catalase rescues ventricular myocytes from ethanol-induced cardiac contractile defect. *J Mol Cell Cardiol* 35:645–652
- Hintz KK, Relling DP, Saari JT et al (2003) Cardiac overexpression of alcohol dehydrogenase exacerbates cardiac contractile dysfunction, lipid peroxidation, and protein damage after chronic ethanol ingestion. *Alcohol Clin Exp Res* 27:1090–1098
- Dong F, Zhang X, Wold LE, Ren Q, Zhang Z, Ren J (2005) Endothelin-1 enhances oxidative stress, cell proliferation and reduces apoptosis in human umbilical vein endothelial cells: role of ETB receptor, NADPH oxidase and caveolin-1. *Br J Pharmacol* 145:323–333
- Davidoff AJ, Davidson MB, Carmody MW, Davis ME, Ren J (2004) Diabetic cardiomyocyte dysfunction coupled to myocyte insulin resistance: role of glucose-induced PKC activity. *Mol Cell Biochem* 262:155–163
- Matthaei S, Stumvoll M, Kellerer M, Haring HU (2000) Pathophysiology and pharmacological treatment of insulin resistance. *Endocr Rev* 21:585–618
- Ren J, Sowers JR, Walsh MF, Brown RA (2000) Reduced contractile response to insulin and insulin-like growth factor I in ventricular myocytes from genetically obese Zucker rats. *Am J Physiol Heart Circ Physiol* 279:H1708–H1714
- Sharikabad MN, Ostbye KM, Brors O (2004) Effect of hydrogen peroxide on reoxygenation-induced Ca²⁺ accumulation in rat cardiomyocytes. *Free Radic Biol Med* 37:531–538
- Schaffer SW, Ballard-Croft C, Boerth S, Allo SN (1997) Mechanisms underlying depressed Na⁺/Ca²⁺ exchanger activity in the diabetic heart. *Cardiovasc Res* 34:129–136
- Shimoni Y, Ewart HS, Severson D (1998) Type I and II models of diabetes produce different modifications of K⁺ currents in rat heart: role of insulin. *J Physiol* 507:485–496
- Goldhaber JJ, Henderson SA, Reuter H, Pott C, Philipson KD (2005) Effects of Na⁺-Ca²⁺ exchange expression on excitation-contraction coupling in genetically modified mice. *Ann NY Acad Sci* 1047:122–126

31. Bers DM (2002) Cardiac excitation–contraction coupling. *Nature* 415:198–205
32. Ren J, Duan J, Hintz KK, Ren BH (2003) High glucose induces cardiac insulin-like growth factor I resistance in ventricular myocytes: role of Akt and ERK activation. *Cardiovasc Res* 57:738–748
33. Huisamen B (2003) Protein kinase B in the diabetic heart. *Mol Cell Biochem* 249:31–38
34. Tomas E, Lin YS, Dagher Z et al (2002) Hyperglycemia and insulin resistance: possible mechanisms. *Ann NY Acad Sci* 967:43–51
35. Ren J, Zhang X, Scott GI et al (2004) Adenovirus gene transfer of recombinant eNOS enhances contractile function in ventricular myocyte. *J Cardiovasc Pharm* 43:171–177
36. Meng TC, Buckley DA, Galic S, Tiganis T, Tonks NK (2004) Regulation of insulin signaling through reversible oxidation of the protein-tyrosine phosphatases TC45 and PTP1B. *J Biol Chem* 279:37716–37725
37. Miatello R, Risler N, Castro C, Gonzalez S, Ruttler M, Cruzado M (2001) Aortic smooth muscle cell proliferation and endothelial nitric oxide synthase activity in fructose-fed rats. *Am J Hypertens* 14:1135–1141
38. Stockklauser-Farber K, Ballhausen T, Laufer A, Rosen P (2000) Influence of diabetes on cardiac nitric oxide synthase expression and activity. *Biochim Biophys Acta* 1535:10–20
39. Penckofer S, Schwertz D, Florczak K (2002) Oxidative stress and cardiovascular disease in type 2 diabetes: the role of antioxidants and pro-oxidants. *J Cardiovasc Nurs* 16:68–85
40. Cavarape A, Feletto F, Mercuri F, Quagliaro L, Daman G, Ceriello A (2001) High-fructose diet decreases catalase mRNA levels in rat tissues. *J Endocrinol Invest* 24:838–845
41. Blendea MC, Jacobs D, Stump CS et al (2005) Abrogation of oxidative stress improves insulin sensitivity in the Ren2 rat model of tissue angiotensin II overexpression. *Am J Physiol Endocrinol Metab* 288:E353–E359